

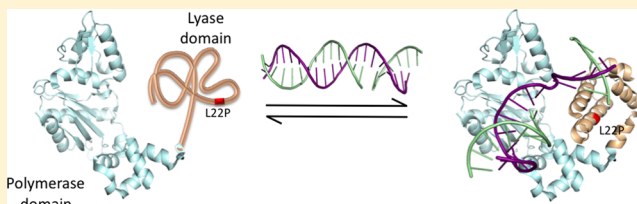
# Substrate Rescue of DNA Polymerase $\beta$ Containing a Catastrophic L22P Mutation

Thomas W. Kirby, Eugene F. DeRose, William A. Beard, David D. Shock, Samuel H. Wilson, and Robert E. London\*

Laboratory of Structural Biology, National Institute of Environmental Health Sciences, Research Triangle Park, North Carolina 27709, United States

## Supporting Information

**ABSTRACT:** DNA polymerase (pol)  $\beta$  is a multidomain enzyme with two enzymatic activities that plays a central role in the overlapping base excision repair and single-strand break repair pathways. The high frequency of pol  $\beta$  variants identified in tumor-derived tissues suggests a possible role in the progression of cancer, making the determination of the functional consequences of these variants of interest. Pol  $\beta$  containing a proline substitution for leucine 22 in the lyase domain (LD), identified in gastric tumors, has been reported to exhibit severe impairment of both lyase and polymerase activities. Nuclear magnetic resonance (NMR) spectroscopic evaluations of both pol  $\beta$  and the isolated LD containing the L22P mutation demonstrate destabilization sufficient to result in LD-selective unfolding with minimal structural perturbations to the polymerase domain. Unexpectedly, addition of single-stranded or hairpin DNA resulted in partial refolding of the mutated lyase domain, both in isolation and for the full-length enzyme. Further, formation of an abortive ternary complex using  $\text{Ca}^{2+}$  and a complementary dNTP indicates that the fraction of pol  $\beta$ (L22P) containing the folded LD undergoes conformational activation similar to that of the wild-type enzyme. Kinetic characterization of the polymerase activity of L22P pol  $\beta$  indicates that the L22P mutation compromises DNA binding, but nearly wild-type catalytic rates can be observed at elevated substrate concentrations. The organic osmolyte trimethylamine *N*-oxide (TMAO) is similarly able to induce folding and kinetic activation of both polymerase and lyase activities of the mutant. Kinetic data indicate synergy between the TMAO cosolvent and substrate binding. NMR data indicate that the effect of the DNA results primarily from interaction with the folded LD(L22P), while the effect of the TMAO results primarily from destabilization of the unfolded LD(L22P). These studies illustrate that substrate-induced catalytic activation of pol  $\beta$  provides an optimal enzyme conformation even in the presence of a strongly destabilizing point mutation. Accordingly, it remains to be determined whether this mutation alters the threshold of cellular repair activity needed for routine genome maintenance or whether the “inactive” variant interferes with DNA repair.



The genetic instability that leads to the development of cancer is driven by the accumulation of damaged DNA. Impairment of any of the DNA repair pathways represents one mechanism leading to such an accumulation.<sup>1,2</sup> Approximately 30% of human tumors that have been sequenced show variations in DNA polymerase (pol)  $\beta$ , an enzyme that is centrally important in the overlapping base excision repair (BER) and single-strand break repair pathways.<sup>3–5</sup> A large number of tumor-associated mutations in pol  $\beta$  have been identified, and the functional effects of many of them have been characterized.<sup>6–12</sup> Many of these mutations confer mutator phenotypes on the enzyme, and several of these cancer-associated mutations have catastrophic effects on enzymatic activity.<sup>13,14</sup> The pol  $\beta$ (E295K) mutation alters a critical residue in the sensor–effector coupling pathway that constitutes the functional connection between correct base pair sensing and catalytic activation. Recent nuclear magnetic resonance (NMR) studies of pol  $\beta$ (E295K) demonstrate the failure of a correctly matched ternary complex to induce the conformationally

activated state,<sup>13</sup> a result consistent with the extremely low activity found for this mutant.<sup>10</sup>

In addition to impairing activity, some mutated forms of pol  $\beta$  can have additional consequences resulting from non-productive binding of damaged DNA intermediates or the displacement of native, wild-type pol  $\beta$  from DNA repair complexes. Pol  $\beta$  is known to form a specific complex with the amino-terminal domain of the scaffold X-ray cross complementing group 1 protein (XRCC1) involving the carboxyl-terminal “N-subdomain” of the enzyme.<sup>15,16</sup> Mutations that influence pol  $\beta$  structure or activity but leave the interface with XRCC1 unperturbed can interfere with the normal function of the repair complex. Thus, a binary complex formed between a truncated pol  $\beta$ , pol  $\beta\Delta_{208–236}$ , and XRCC1 acts as a dominant-negative mutant, and transgenic mice expressing the truncated

Received: February 11, 2014

Revised: March 20, 2014

Published: March 21, 2014

form of pol  $\beta$  exhibit a significantly elevated incidence of tumor formation.<sup>17</sup>

Pol  $\beta$  containing the L22P mutation in the lyase domain (LD) has been identified in cells derived from a gastric carcinoma.<sup>6,9</sup> The mutation was found to significantly impair both enzymatic activities; pol  $\beta$  (L22P) exhibits negligible 5'-deoxyribose phosphate (dRP) lyase activity, and very low<sup>6</sup> or no<sup>14</sup> polymerase activity. Molecular dynamics simulations indicated that the L22P mutant is characterized by altered packing that results in considerable destabilization.<sup>6</sup> In our study, we have utilized NMR spectroscopy to evaluate the structural impact of the L22P mutation. We also have evaluated the effects of the mutation on enzyme activity and substrate binding, as well as the structural effects of substrate interactions on the L22P-perturbed enzyme structure.

## EXPERIMENTAL PROCEDURES

**Proteins.** [methyl-<sup>13</sup>C]Methionine-labeled pol  $\beta$  (L22P) and pol  $\beta$  (L22P)LD (residues 1–87) were prepared as described previously<sup>21</sup> by growth of plasmid-containing *Escherichia coli* on a medium containing [methyl-<sup>13</sup>C]methionine (CIL, Cambridge, MA). The [U-<sup>2</sup>H], [Ile- $\delta$ -<sup>13</sup>CH<sub>3</sub>] samples were expressed in *E. coli* BL21(DE)3 transformants grown in M9 deuterated (99% D<sub>2</sub>O) medium containing [U-<sup>2</sup>H,<sup>13</sup>C]glycerol and <sup>15</sup>NH<sub>4</sub>Cl as the sole carbon and nitrogen sources, respectively; 50 mg per liter of [3,3'-<sup>2</sup>H<sub>2</sub>,1,2,3,4-<sup>13</sup>C<sub>4</sub>]- $\alpha$ -ketobutyric acid was added to the deuterated culture 30 min prior to protein induction by the addition of isopropyl  $\beta$ -D-1-thiogalactopyranoside. The L22P variants were generated using the QuikChange kit (Stratagene). The protein concentrations were determined using 280 nm extinction coefficients of 20088 M<sup>-1</sup> cm<sup>-1</sup> for full-length polymerases and 3591 M<sup>-1</sup> cm<sup>-1</sup> for the isolated lyase domains.

**Oligonucleotides.** Oligonucleotides for NMR (from Oligoset or IDT) were dissolved in D<sub>2</sub>O to make an ~10 mM stock solution. The single-stranded DNA used for the NMR experiments has a 5'-CCG ACG GCG CAT CAG C-3' sequence. The short hairpin DNA used for the NMR experiments has a 5'-<sup>P</sup>CTG GCG AAG CCA G-3' sequence. The double-hairpin, one-nucleotide gap DNA substrate used for the NMR experiments has a 5'-<sup>P</sup>GGC GAA GCC TGG TGC GAA GCA CC-3' sequence (the templating T in the gap is underlined). The DNA concentrations were determined using their 260 nm extinction coefficients. The oligonucleotides used to construct substrates for single-nucleotide gap-filling reactions were the 5'-6-carboxyfluorescein labeled primer (5'-CTG CAG CTG ATG CGC-3'), the downstream oligonucleotide (5'-GTA CGG ATC CCC GGG TAC-3'), and the template (3'-GAC GTC GAC TAC GCG GCA TGC CTA GGG GCC CAT G-5', where the templating G in the gap is underlined). The downstream oligonucleotide was synthesized with a 5'-phosphate. The oligonucleotides used to construct substrates to assay removal of a 5'-dRP group were the primer (5'-CAT ATC CGT GTC GCC CTC-3'), the downstream oligonucleotide (5'-U ATT CCG ATA GTG ACT ACA-6-carboxyfluorescein-3'), and the template (3'-GTA TAG GCA CAG CGG GAG TAA GGC TAT CAC TGA TGT-5').

**NMR Spectroscopy.** NMR samples contained 0.1–0.6 mM protein in a buffer (10% D<sub>2</sub>O for <sup>1</sup>H–<sup>15</sup>N HSQC experiments and 100% D<sub>2</sub>O for <sup>1</sup>H–<sup>13</sup>C HSQC and HMQC experiments) consisting of 50 mM Tris-*d*<sub>11</sub> (pH 7.6), 150 mM KCl, 1 mM CDTA, 1 mM dithiothreitol (DTT), 0.1 mM AEBF, 0.04% NaN<sub>3</sub>, and 50  $\mu$ M DSS as an internal chemical shift standard.

NMR experiments were performed at 25 °C on a Varian UNITY INOVA 600 or 800 MHz NMR spectrometer, using a 5 mm Varian <sup>1</sup>H{<sup>13</sup>C,<sup>15</sup>N} triple-resonance room-temperature or cold probe, equipped with actively shielded Z-gradients. The <sup>1</sup>H–<sup>13</sup>C HSQC spectra were recorded using Varian's gChsqc sequence;<sup>22</sup> the <sup>13</sup>C HMQC experiments were performed using Varian's gChmqc sequence. The spectra were processed using NMRPipe version 2.1<sup>23</sup> and analyzed using NMRView version 5.0.4.<sup>24</sup> All spectra were processed using squared cosine bell apodization functions in all dimensions and forward–backward linear prediction in the indirect dimension.<sup>25</sup>

The isoleucine  $\delta$ 1-methyl chemical shift assignments were made on an isoleucine-labeled sample in a 1:1 complex with the one-nucleotide gapped double-hairpin DNA described above in a buffer solution consisting of 100 mM phosphate (pH 6.7), 1 mM CDTA, 1 mM DTT, 0.1 mM AEBF, 0.04% NaN<sub>3</sub>, and 50  $\mu$ M DSS as an internal chemical shift standard. It was determined that the samples were stable for several weeks at 35 °C in the lower-pH phosphate buffer. The higher temperature greatly improved the signal-to-noise ratio of the three-dimensional (3D) chemical shift assignment experiments described below. The backbone chemical shift assignments of this complex were made from a combination of 3D HNCA, HN(CO)CA, HN(CA)CB, HN(COCA)CB, and HNCO experiments<sup>26</sup> and shown to agree for the most part with the assignments of a similar pol  $\beta$ -DNA complex.<sup>27</sup> The isoleucine methyl assignments were made using a combination of 3D Ile,Leu-(HM)CM(CGCB)CA)NH, Ile,Leu-HM-(CMCGCB)CA)NH, HMCM[CG]CB)CA, and Ile,Leu-HMCM(CGCB)CA)CO experiments.<sup>28</sup> The Ile,Leu-(HM)CM-(CGCB)CA)NH and Ile,Leu-HM(CMCGCB)CA)NH experiments were conducted on a Varian Inova 800 MHz spectrometer equipped with a <sup>1</sup>H{<sup>13</sup>C,<sup>15</sup>N} cold probe. All the other 3D experiments were conducted on a Varian Inova 600 MHz spectrometer also equipped with a <sup>1</sup>H{<sup>13</sup>C,<sup>15</sup>N} cold probe.

**DNA Preparation.** DNA substrates for single-nucleotide gap-filling DNA synthesis or dRP lyase activity measurements were prepared by annealing three purified oligonucleotides. Each oligonucleotide was suspended in 10 mM Tris-HCl (pH 7.4) and 1 mM EDTA, and the concentration was determined from their UV absorbance at 260 nm. The annealing reactions were conducted by incubating a solution of primer with downstream and template oligonucleotides (1:1.2:1.2 molar ratio) at 95 °C for 5 min and cooling the sample at a rate of 1 °C/min to 10 °C in a PCR thermocycler.

**Single-Nucleotide Gap-Filling DNA Synthesis.** Steady-state kinetic parameters for single-nucleotide gap-filling reactions at 37 °C were determined by initial velocity measurements as described previously.<sup>29</sup> Unless noted otherwise, enzyme activities were determined using a standard reaction mixture containing 50 mM Tris-HCl (pH 7.4, 37 °C), 100 mM KCl, 10 mM MgCl<sub>2</sub>, 1 mM DTT, 100  $\mu$ g/mL bovine serum albumin, 10% glycerol, and 500 nM single-nucleotide gapped DNA. For reactions with TMAO, glycerol was omitted. Enzyme concentrations and reaction time intervals were chosen so that substrate depletion or product inhibition did not influence initial velocity measurements. Reactions were stopped with EDTA and samples mixed with an equal volume of formamide dye. The substrates and products were separated on 16% denaturing (8 M urea) polyacrylamide gels. Because a 6-carboxyfluorescein 5'-labeled primer was used in these assays, the products were quantified using the GE Typhoon

phosphorimager in fluorescence mode. Steady-state kinetic parameters were determined by fitting the rate data to the Michaelis equation. When the observed rates could not be saturated because of poor substrate binding, the data were fit to an alternate form of the Michaelis equation to extract the apparent catalytic efficiency ( $k_{\text{cat}}/K_M$ , best-fit initial slope).

$$k_{\text{obs}} = [(k_{\text{cat}}/K_M)S]/(1 + S/K_M) \quad (1)$$

**dRP Lyase Activity.** To generate a 5'-dRP group, the annealed DNA substrate with a 5'-uracil on the downstream oligonucleotide was treated with 50 nM uracil DNA glycosylase for 30 min at 37 °C. The DNA substrate was stored on ice until it was used. Prior to being used, the DNA substrate was incubated at 37 °C for 5 min before initiation of the reaction with enzyme. The reaction mixture included 50 mM HEPES-KOH (pH 7.5), 20 mM KCl, 0.5 mM EDTA, 1 mM DTT, 10% glycerol, and 100 nM DNA. For reactions with TMAO, glycerol was omitted. Reactions were quenched with freshly prepared cold 200 mM NaBH<sub>4</sub> (final concentration) and mixtures put on ice for at least 30 min. After the mixtures had been briefly heated (5 min at 95 °C), the DNA was resolved on 15% denaturing (8 M urea) polyacrylamide gels. Because a 6-carboxyfluorescein 3'-labeled downstream oligonucleotide was used in these assays, the products were visualized using the GE Typhoon phosphorimager in fluorescence mode.

## RESULTS

It has been reported that pol  $\beta$ (L22P) exhibits no lyase activity and negligible polymerase activity,<sup>6,14</sup> so that it was anticipated that the L22P substitution would significantly perturb the NMR resonances of the pol  $\beta$  lyase domain. A comparison of the <sup>1</sup>H-<sup>15</sup>N HSQC spectra obtained for pol  $\beta$ (L22P) with that of pol  $\beta$  reveals that the amide resonances of the catalytic domain show negligible or small chemical shift perturbations, while the amide resonances of the lyase domain are largely absent (Figure 1A,B). The spectra also contain additional intense resonances consistent with substantial, domain-specific unfolding. In harmony with these observations, the <sup>1</sup>H-<sup>15</sup>N HSQC spectrum obtained for the isolated mutant pol  $\beta$  lyase domain, LD(L22P), is generally consistent with expectations for a random coil (Figure 1C); the <sup>1</sup>H shift range of the amide protons is mostly localized to the region between ~8 and 8.5 ppm.<sup>30</sup> Some resonance broadening is observed, suggesting a dynamic state that may include regions containing some degree of secondary structure. In contrast with these results, the spectrum of the wild-type LD exhibits dispersion typical of a folded domain (Figure 1C).

Previous NMR studies of pol  $\beta$  containing <sup>13</sup>C-labeled methyl groups have proven to be particularly useful for the analysis of substrate binding and conformational activation.<sup>13,31,32</sup> The region of the <sup>1</sup>H-<sup>13</sup>C HSQC spectrum containing the isoleucine  $\delta$ -methyl resonances of binary complexes of pol  $\beta$  or the L22P variant with a double-hairpin gapped DNA substrate is shown in Figure 2A. The  $\delta$ -<sup>13</sup>CH<sub>3</sub>-Ile resonances in the LD annotated with blue numbers are essentially missing for the L22P mutant, consistent with the conclusions regarding the loss of structure described above. Alternatively, the  $\delta$ -<sup>13</sup>CH<sub>3</sub>-Ile resonances in the polymerase domain are unaffected (black annotations) or, in some cases, show small but significant shift perturbations (magenta annotations). Importantly, the latter resonances overlay quite well with resonances from uncomplexed wild-type pol  $\beta$ ,

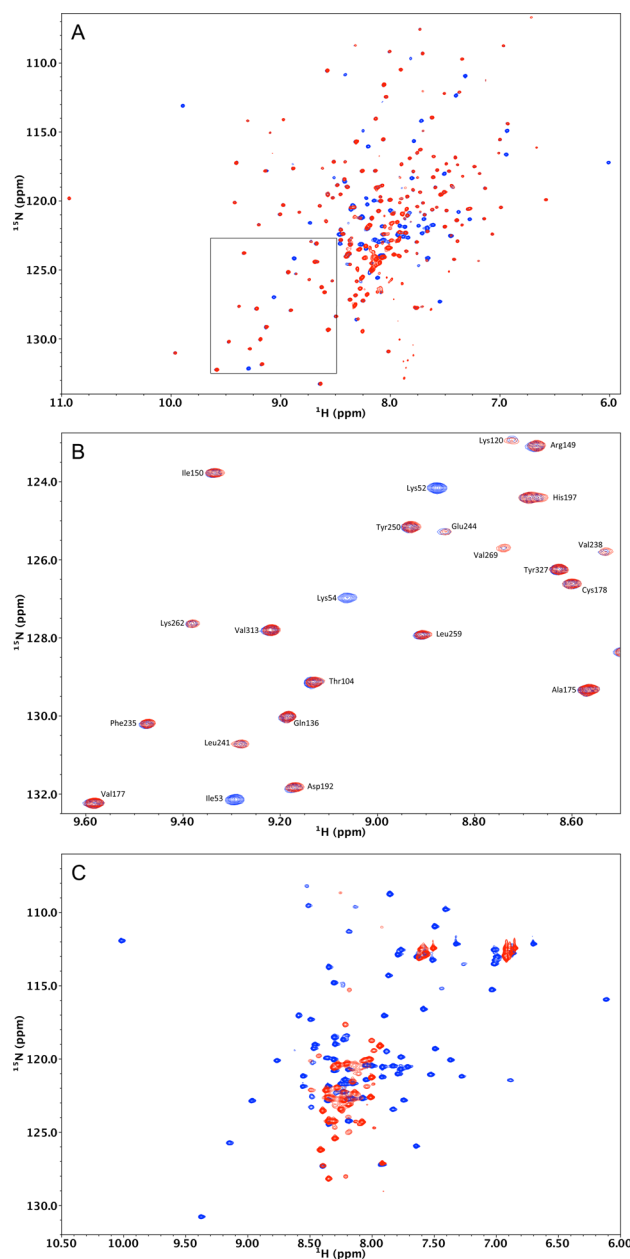


**Figure 1.** Effects of the L22P mutation on amide resonances of pol  $\beta$ . (A) Overlay of the <sup>1</sup>H-<sup>15</sup>N HSQC spectra of 130  $\mu$ M [U-<sup>2</sup>H,<sup>15</sup>N]pol  $\beta$  (blue) and 116  $\mu$ M [<sup>2</sup>H,<sup>15</sup>N]pol  $\beta$ (L22P) (red). (B) Expansion of the boxed region showing the disappearance of lyase domain resonances. (C) Overlay of the <sup>1</sup>H-<sup>15</sup>N HSQC spectra of 100  $\mu$ M [U-<sup>2</sup>H,<sup>15</sup>N]LD (blue) and 100  $\mu$ M [<sup>2</sup>H,<sup>15</sup>N]LD(L22P) (red). All samples were in 50 mM Tris-*d*<sub>11</sub> (pH 7.6), 150 mM KCl, 1 mM CDTA, 10 mM NaN<sub>3</sub>, and 10% D<sub>2</sub>O. Spectra were recorded at 25 °C.

indicating that there is very little binding of the double-hairpin substrate by the mutant enzyme (Figure 2B). Thus, the apparent indirect chemical shift perturbations of the isoleucine 106, 119, 138, 257, 260, and 277 resonances resulting from the L22P mutation can all be explained by the loss of DNA binding and the accompanying loss of the DNA-induced conformational perturbations (Figure 2C). Interestingly, the  $\delta$ -<sup>13</sup>CH<sub>3</sub> resonance for Ile97, corresponding to a residue on  $\alpha$ -helix F, has also disappeared and is annotated in blue (Figure 2A). Although this helix is typically assigned to the DNA-binding subdomain, it interacts closely with helices A and E in the LD,



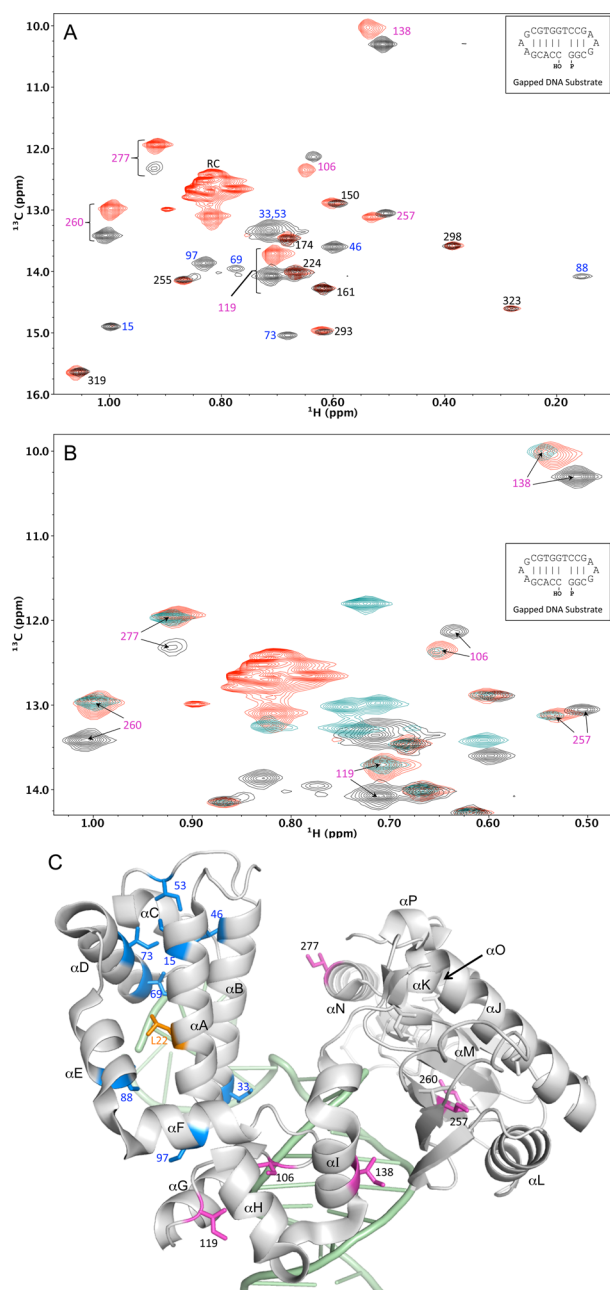


**Figure 2.** Effect of the L22P mutation on pol  $\beta$  Ile methyl resonances. (A)  $^1\text{H}$ – $^{13}\text{C}$  HSQC spectral overlay corresponding to binary complexes of  $[\delta\text{-}^{13}\text{CH}_3\text{-Ile}]\text{pol } \beta$  (black) and  $[\delta\text{-}^{13}\text{CH}_3\text{-Ile}]\text{pol } \beta(\text{L22P})$  (red) with a one-nucleotide gapped double-hairpin DNA substrate. Resonances experiencing large shifts (presumably to the random coil positions) are annotated in blue, and resonances experiencing smaller shifts are annotated in magenta. (B) Expansion of the HSQC spectrum shown in panel A with an additional overlay of apoenzyme  $[\delta\text{-}^{13}\text{CH}_3\text{-Ile}]\text{pol } \beta$  (teal), illustrating that most of the Ile resonance shifts in the polymerase domain do not result directly from the mutation but are indirect consequences of weakened DNA binding. (C) Structure of the pol  $\beta$ -DNA ternary complex (Protein Data Bank entry 3ISD) showing the residues whose resonances are affected by the L22P (orange) mutation. Blue and magenta residues in panel C correspond to blue and magenta annotations in panel A, respectively. All samples were in 50 mM Tris- $d_{11}$  (pH 7.6), 150 mM KCl, 1 mM CDTA, 10 mM  $\text{NaN}_3$ , and 100%  $\text{D}_2\text{O}$ . Spectra were recorded at 25  $^\circ\text{C}$ .

so it is not surprising that the catastrophic loss of structure of the LD should significantly affect a residue on  $\alpha$ -helix F. Examination of the well-resolved amide resonances of the variant enzyme indicates disappearance for residues 99 and 100, but not residue 104, suggesting that from a structural standpoint, the integrity and positioning of  $\alpha$ -helix F are strongly dependent on the presence of a folded LD.

**Interaction of DNA with the Pol  $\beta$  LD.** The amino-terminal LD of pol  $\beta$  has a pI of 10.4 and a high affinity for both single- and double-stranded DNA.<sup>33</sup> As shown previously, the methionine methyl resonances in pol  $\beta$  provide useful indicators of both ligand binding and conformational activation, with Met18 specifically sensing interactions with the DNA located immediately downstream of the single-nucleotide gap.<sup>31</sup> As expected from the behavior of amide resonances discussed above, the Met18 methyl resonance of LD(L22P) is strongly shifted from its position in the wild-type domain, exhibiting an intense peak at  $\delta(^1\text{H}, ^{13}\text{C}) = (2.07, 16.97)$ , close to the expected position for a methionine methyl resonance in a random coil peptide<sup>30</sup> (Figure 3A). In the presence of excess ssDNA, a second, considerably less intense resonance is observed at  $\delta(^1\text{H}, ^{13}\text{C}) = (1.66, 16.08)$  close to the position of the Met18 resonance in the wild-type LD (Figure 3B). Further addition of ssDNA leads to only minimal changes, indicating that the stabilization resulting from ssDNA binding is insufficient to fully compensate for the destabilization produced by the L22P mutation. Analogous results were obtained using hairpin DNA, similar in structure to those used in our previous studies (Figure 3C).<sup>32,34</sup> Although the intensity of the shifted Met18 resonance in the DNA-LD(L22P) complex is considerably lower than that of the resonance in the uncomplexed domain, the fraction of folded LD(L22P) is higher than a direct comparison of the intensities would indicate, because of the relaxation differences between the folded and unfolded conformations.

#### Effects of TMAO on the Conformation of the LD.

TMAO is a naturally occurring organic osmolyte that has been shown to promote protein folding by destabilizing the unfolded state.<sup>18</sup> Titration of a sample of  $[\text{U-}^{13}\text{CH}_3\text{-Met}]\text{LD}$  with TMAO results in a loss of intensity of the random coil Met18 resonance, and a parallel increase in the intensity of a broad resonance near the folded position (Figure 3D). Interestingly, the TMAO titration does not produce a concentration-dependent shift perturbation, but rather a shift in the ratio of intensities of the two observed methionine methyl resonances. These results are consistent with a two-state conformational equilibrium of the LD(L22P), in which the primary effect of the TMAO is to alter the relative stability of the two component states. In comparison with the effects of the DNA ligands shown in panels B and C of Figure 3, the TMAO-induced Met18 resonance is broader and further shifted from its position in the wild-type LD, and the Met18 peak at the random coil position is much more effectively eliminated. Despite these changes suggesting that TMAO promotes folding of the LD(L22P) to a conformation similar to that of the wild-type domain, the  $^1\text{H}$ – $^{15}\text{N}$  HSQC spectrum of the  $[\text{U-}^{15}\text{N}]\text{-LD(L22P)}$  shows considerably less dispersion and uniformity than the spectrum of the domain lacking the mutation (Figure S1 of the Supporting Information). In general, the effects observed are consistent with studies indicating that the primary effect of TMAO is destabilization of the random coil form of the domain as a result of unfavorable interactions between the TMAO and the peptide backbone.<sup>18,19,35</sup>

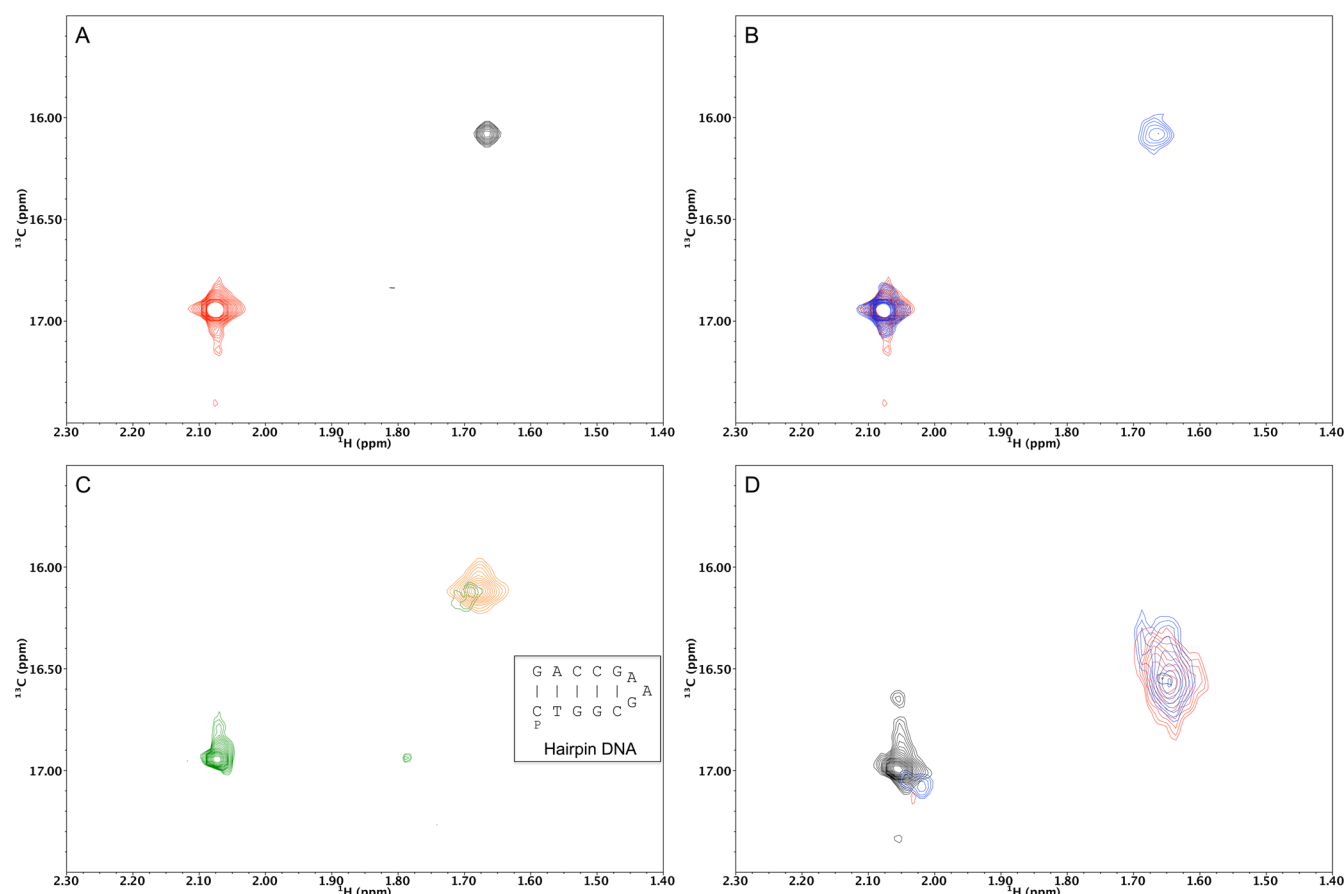


**Figure 3.** Effects of DNA and TMAO on the Met18 resonance of the isolated pol  $\beta$  lyase domain. (A) Overlaid  $^1\text{H}$ – $^{13}\text{C}$  HSQC spectra of  $[^{13}\text{CH}_3\text{-Met}]$ LD (black) and  $[^{13}\text{CH}_3\text{-Met}]$ LD(L22P) (red). (B) Overlaid  $^1\text{H}$ – $^{13}\text{C}$  HSQC spectra of  $[^{13}\text{CH}_3\text{-Met}]$ LD(L22P) in the absence (red) or presence (blue) of 187  $\mu\text{M}$  ssDNA. (C) Overlaid  $^1\text{H}$ – $^{13}\text{C}$  HSQC spectra of  $[^{13}\text{CH}_3\text{-Met}]$ LD (orange) and  $[^{13}\text{CH}_3\text{-Met}]$ LD(L22P) in the presence of 411  $\mu\text{M}$  hairpin DNA (green). (D) Overlaid  $^1\text{H}$ – $^{13}\text{C}$  HSQC spectra of  $[^{13}\text{CH}_3\text{-Met}]$ LD(L22P) in the presence of 1, 2, or 3 M TMAO (black, blue, or red, respectively). All spectra correspond to  $100 \pm 12 \mu\text{M}$  LD in 50 mM Tris- $d_{11}$  (pH 7.6), 150 mM KCl, 1 mM CDTA, 10 mM  $\text{NaN}_3$ , and 100%  $\text{D}_2\text{O}$ . Spectra were recorded at 25  $^\circ\text{C}$ .

### Substrate-Induced Folding and Conformational Activation of Pol $\beta$ (L22P).

In response to the addition of its substrates, pol  $\beta$  undergoes a series of conformational changes that are conveniently monitored with the methionine methyl resonances.<sup>31</sup> The  $^1\text{H}$ – $^{13}\text{C}$  spectrum of  $[^{13}\text{CH}_3\text{-Met}]$ pol  $\beta$ (L22P) is very similar to that of the wild-type enzyme, except that the Met18 resonance typically observed at  $\delta(^1\text{H}, ^{13}\text{C}) = (1.66, 16.10)$  is replaced by an intense resonance at  $\delta(^1\text{H}, ^{13}\text{C}) = (2.08, 16.97)$ , as seen for the isolated LD (Figure 4, black spectrum). Addition of a single-nucleotide gapped double-hairpin DNA substrate to  $[^{13}\text{CH}_3\text{-Met}]$ pol  $\beta$ (L22P) produces a typical, small shift of the Met236 resonance. For Met18, two resonances are observed: a sharp and intense resonance near the random coil position and a broader resonance near the position expected for Met18 in the wild-type DNA complex (Figure 4, red spectrum). On the basis of comparisons of the methionine resonance intensities, we estimate that in the presence of the double-hairpin DNA, ~20% of the pol  $\beta$ (L22P) has adopted a folded state approximating that of the wild-type enzyme. Because the DNA-stabilized pol  $\beta$ (L22P) contains the mutation, the substrate-rescued conformation is expected to approximate rather than duplicate that of the wild-type enzyme.

Next, an abortive ternary complex was formed by addition of complementary dATP and  $\text{CaCl}_2$  to the binary pol  $\beta$ (L22P)·DNA complex (Figure 4, blue spectrum). This strategy

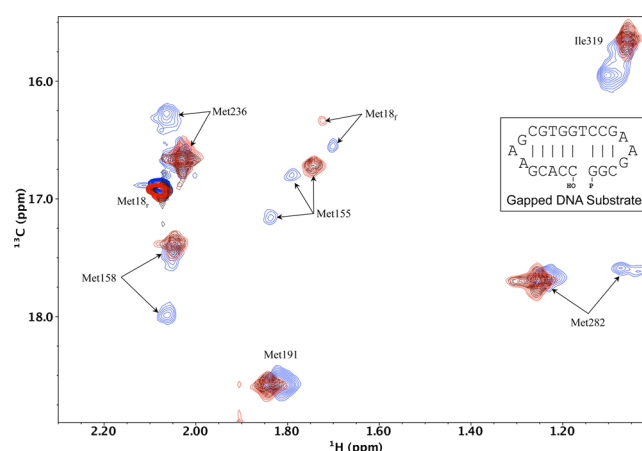


**Figure 4.** Effects of substrates on methionine resonances of pol  $\beta$ (L22P). Overlaid  $^1\text{H}$ – $^{13}\text{C}$  HSQC spectra correspond to 100  $\mu\text{M}$   $[^{13}\text{CH}_3\text{-Met}]$ pol  $\beta$ (L22P) alone (black) and after addition of 119  $\mu\text{M}$  one-nucleotide gapped double-hairpin DNA (red) and further addition of 500  $\mu\text{M}$  dATP in the presence of 10 mM  $\text{CaCl}_2$  (blue). Samples were in 50 mM Tris- $d_{11}$ , 150 mM KCl, 1 mM CDTA, 10 mM  $\text{NaN}_3$  (pH 7.6), and 100%  $\text{D}_2\text{O}$  and run at 25  $^\circ\text{C}$ .

represents an alternative to that used previously, in which gap-filling synthesis was blocked using either a dideoxy-

terminated primer or a nonhydrolyzable dNTP analogue.<sup>31,32</sup> The use of  $\text{Ca}^{2+}$  represents an attractive alternative because it promotes a ternary complex with the true enzyme substrates but fails to support catalysis.<sup>36</sup> Although in the binary complex only the Met18 resonance exhibits two peaks, formation of the ternary complex results in two sets of resonances for each methionine methyl group, except for Met191. The methionine resonance shifts indicate that in the presence of these substrates, the fraction of the pol  $\beta$ -DNA-dATP ternary complex in which the LD has been conformationally rescued by the DNA substrate undergoes further conformational activation similar to that of the wild-type ternary complex. In particular, the abortive ternary complex is characterized by a downfield shift of the Met158 resonance in the  $^{13}\text{C}$  dimension, and an upfield shift of the Met282 resonance in the  $^1\text{H}$  dimension. As discussed previously, this  $^1\text{H}$  shift is consistent with the transition to a closed enzyme conformation and the increased proximity of the Met282 methyl group to Phe320.<sup>32</sup> Although in previous studies of the wild-type enzyme, the Met18 resonance was observed to respond to the DNA substrate but not to the formation of the ternary complex, the Met18 resonance of pol  $\beta$ (L22P) undergoes an additional shift change upon ternary complex formation (Figure 4). Apparently, the reduced stability of the LD in the mutant enzyme makes the domain conformation more susceptible to the perturbation produced by ternary complex formation.

One other characteristic worth noting is the observation of a shifted Met155 resonance in the ternary complex. Previous studies of Mg-containing ternary complexes did not result in an observable Met155 peak, which was too severely broadened to permit unequivocal observation. In contrast, the  $\text{Ca}^{2+}$ -containing ternary complex appears to provide greater stabilization of the closed enzyme conformation, so that the shifted resonance for Met155 can be observed. This observation is independent of the presence of the L22P mutation, and we have made similar observations in other studies of  $\text{Ca}^{2+}$ -containing pol  $\beta$  ternary complexes (unpublished results). For the  $\text{Ca}^{2+}$  ternary complex, Met191 is also subject to a small resonance shift. Overall, these studies demonstrate that the DNA substrate is able to induce a folded conformation of the mutated LD that approximates that of the wild-type enzyme. Formation of an abortive ternary complex is then able to induce the conformationally activated state in a fraction of the substrate-rescued enzyme. A larger fraction of the enzyme contains an apparently unfolded LD, binds DNA poorly, and fails to undergo conformational activation (Figure 4).

A comparison of the  $^1\text{H}$ - $^{13}\text{C}$  HSQC spectra obtained for ternary complexes of the wild-type and L22P [ $^{13}\text{CH}_3$ -Met]pol  $\beta$  mutant is shown in Figure 5. In both cases, the abortive ternary complex is produced by addition of double-hairpin DNA forming a single-nucleotide gap with a templating thymine base, dATP, and  $\text{CaCl}_2$ . Under the conditions used in this study, the entire ternary pol  $\beta$  complex exhibits the resonance characteristics of the conformationally activated state. In contrast, the methionine methyl resonances in the pol  $\beta$ (L22P)-DNA- $\text{Ca}^{2+}$ dATP complex are split into two components that we assign to species containing either the disordered or the folded LD. In the complex formed with wild-type pol  $\beta$ , the resonances arising from Met155, Met158, and Met282 are all shifted to positions that correspond to the closed enzyme structure, while in the complex formed with the L22P mutant, each of these residues gives rise to both a shifted resonance and

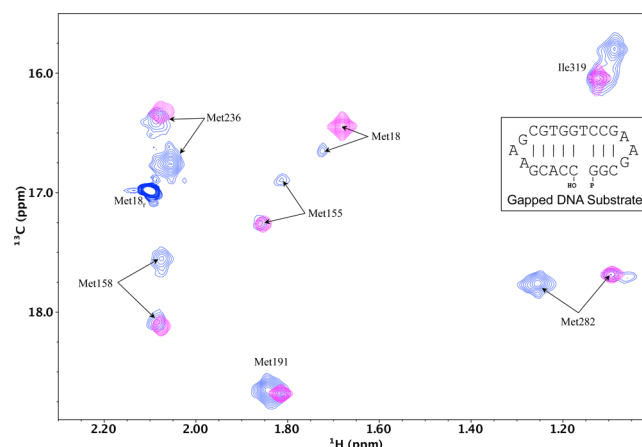


**Figure 5.** Spectral comparison of abortive ternary complexes of wild-type and L22P pol  $\beta$ . Overlaid  $^1\text{H}$ - $^{13}\text{C}$  HSQC spectra of 100  $\mu\text{M}$  [ $^{13}\text{CH}_3$ -methionine]-labeled pol  $\beta$  with a one-nucleotide gap DNA substrate and dATP in the presence of  $\text{CaCl}_2$  (magenta) and 100  $\mu\text{M}$  [ $^{13}\text{CH}_3$ -methionine]-labeled pol  $\beta$  L22P variant with a one-nucleotide gap DNA substrate and dATP in the presence of  $\text{CaCl}_2$  (blue). Samples were in 50 mM Tris- $d_{11}$  (pH 7.6), 150 mM KCl, 1 mM CDTA, 10 mM  $\text{NaN}_3$  (pH 7.6), and 100%  $\text{D}_2\text{O}$  and run at 25  $^\circ\text{C}$ .

an unshifted resonance. For these three pairs of resonances, the intensity ratio of the shifted to unshifted peaks provides an estimate of the fraction of active to inactive enzyme complex. Evaluation of peak intensities is consistent with  $\sim 20$ – $40\%$  folded enzyme complex.

**Effect of the L22P Mutation on DNA Synthesis and dRP Lyase Activities.** Not unexpectedly, the L22P mutant exhibits very low activity when it is assayed at substrate concentrations that would saturate the wild-type enzyme. However, attempts to measure steady-state kinetic constants showed that the activity of the mutant enzyme increases approximately linearly with increasing DNA and dNTP concentrations, reaching a level similar to that of the saturated wild-type enzyme (Figure 6). This behavior is consistent with a DNA binding defect in pol  $\beta$ (L22P) rather than a nucleotide insertion deficiency. The loss of catalytic efficiency can be completely ascribed to the higher apparent  $K_{\text{M,dNTP}}$  characterizing the mutant enzyme (Table 1). An increase in  $K_{\text{M,dNTP}}$  is expected for a DNA polymerase that binds DNA more weakly (i.e., lower processivity because of an increase in its dissociation rate constant).<sup>37</sup> Although it is difficult to saturate the L22P mutant with substrates, an apparent catalytic efficiency ( $k_{\text{cat}}/K_{\text{M,dCTP}}$ ) can be easily quantified. In the presence of 1  $\mu\text{M}$  DNA, the apparent efficiency is  $0.69 \times 10^{-3} \mu\text{M}^{-1} \text{s}^{-1}$ , more than 1000-fold lower than that of wild-type pol  $\beta$  [dG-dCTP (Table 1)].

The amino-terminal LD is responsible for targeting pol  $\beta$  to gapped DNA substrates bearing a 5'-phosphate or dRP group.<sup>38</sup> During base excision repair, the LD removes the 5'-dRP group generating a 5'-phosphate required for DNA ligation after DNA gap-filling synthesis. The destabilizing effect of the L22P mutation on the structure of the LD would also be expected to strongly reduce the dRP lyase activity of pol  $\beta$ . A qualitative dRP activity assay indicates that while activity is reduced, it is not eliminated (Figure 7). This residual activity is consistent with DNA-induced folding of the mutated domain.

Because TMAO appears to stabilize the folded form of the lyase domain of the mutant enzyme, activity was measured in the presence of TMAO. In the presence of 1 M TMAO, steady-

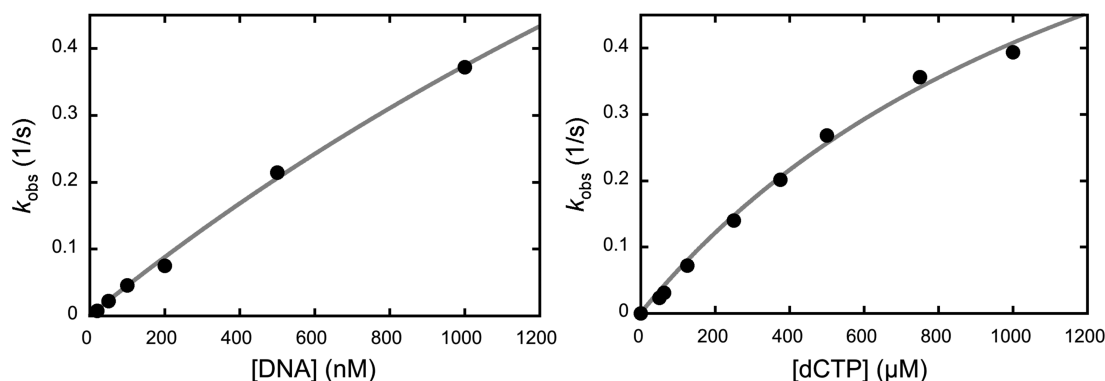


**Figure 6.** Steady-state kinetic characterization of pol  $\beta$ (L22P). The left panel shows the DNA concentration dependence of the observed rate of insertion of dCMP opposite guanine in a single-nucleotide gapped DNA substrate. The concentration of dCTP was 1 mM. The right panel shows the dCTP concentration dependence of the observed rate of insertion of dCMP opposite guanine. The concentration of the single-nucleotide gapped DNA substrate was 1  $\mu$ M. Because the observed rate increased in an approximately linear fashion with substrate concentration, the data were fit to a hyperbolic equation to extract the best-fit initial slope (i.e., apparent catalytic efficiency, gray line; see Experimental Procedures).

**Table 1. Steady-State Kinetic Parameters for Single-Nucleotide Gap-Filling DNA Synthesis<sup>a</sup>**

enzyme	incoming nucleotide	TMAO (1 M)	$K_{M,dNTP}$ ( $\mu$ M)	$k_{cat}$ ( $s^{-1}$ )	$k_{cat}/K_{M,dNTP}$ ( $\times 10^{-3} \mu M^{-1} s^{-1}$ )	fidelity <sup>b</sup>
WT <sup>c</sup>	dCTP	–	1.18 (0.08)	0.96 (0.07)	814 (80)	–
WT	dCTP	+	0.26 (0.07)	0.26 (0.06)	1000 (355)	–
WT	TTP	–	ND <sup>d</sup>	ND <sup>d</sup>	0.08 (0.02)	10175
WT	TTP	+	125 (25)	0.088 (0.002)	0.7 (0.1)	1430
L22P	dCTP	–	ND <sup>d</sup>	ND <sup>d</sup>	0.69	–
L22P	dCTP	+	38 (2)	0.51 (0.03)	13 (1)	–
L22P	TTP	–	NA <sup>e</sup>	NA <sup>e</sup>	NA <sup>e</sup>	NA <sup>e</sup>
L22P	TTP	+	ND <sup>d</sup>	ND <sup>d</sup>	0.0042	3100

<sup>a</sup>The templating base in the gap is guanine. When standard errors are given, the results represent the mean of at least two independent determinations. <sup>b</sup>Fidelity =  $[(k_{cat}/K_{M,dCTP})/(k_{cat}/K_{M,dTTP})]$ . <sup>c</sup>Wild-type enzyme. <sup>d</sup>Not determined because of weak substrate binding. In this situation, the concentration dependence of the observed activities was fit to eq 1. <sup>e</sup>No activity was observed.

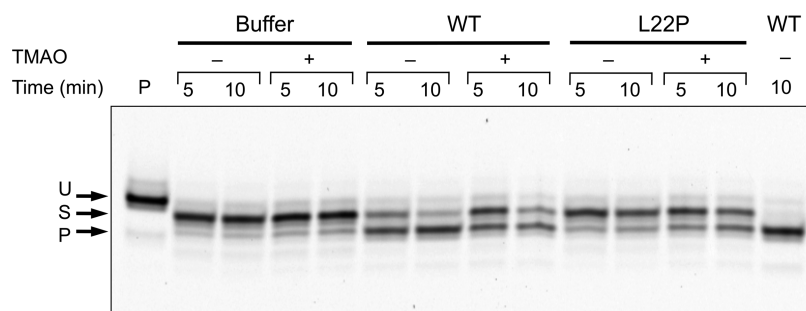


**Figure 7.** Influence of TMAO on the dRP lyase activity of the wild-type and L22P LD. A 5'-uracil-containing downstream oligonucleotide labeled at its 3'-end with 6-FAM (U, lane D) was treated with uracil DNA glycosylase as described in Experimental Procedures to create a substrate (S) for the dRP lyase reaction. The 5'-terminal dRP-containing oligonucleotide migrates farther than the U-containing strand. Removal of the dRP group results in a shorter product (P). The dRP lyase reaction was monitored for 5 and 10 min in the absence (–) or presence (+) of 2 M TMAO with 50 nM enzyme. The last lane included 500 nM wild-type (WT) enzyme, demonstrating complete conversion of substrate to product.

state kinetic parameters for gap-filling DNA synthesis were easily quantified (Table 1). The apparent binding affinities for substrates are increased significantly, resulting in  $\sim 20$ -fold increases in catalytic efficiencies. Higher concentrations of TMAO do not increase activity. The fidelity [i.e.,  $(k_{cat}/K_{M,dCTP})/(k_{cat}/K_{M,dTTP})]$  of the mutant enzyme is similar to that of the wild-type enzyme in the presence of TMAO, suggesting that the L22P substitution does not influence nucleotide discrimination. Interestingly, the fidelity of the wild-type enzyme is significantly reduced in the presence of TMAO (Table 1; –TMAO, 10175 ; +TMAO, 1430). With respect to dRP lyase activity, the activity of the isolated L22P LD is

increased significantly in the presence of TMAO (Figure 7), whereas the activity of the wild-type LD is moderately decreased.

## DISCUSSION

DNA pol  $\beta$  is composed of two domains that complement its biological function in base excision repair. The amino-terminal 8 kDa LD removes the 5'-deoxyribose phosphate generated after incision by apurinic/apyrimidinic endonuclease during the repair of simple base lesions.<sup>39</sup> The LD recognizes the 5'-phosphate in DNA gaps, thereby targeting the polymerase for gap-filling DNA synthesis. The nucleotidyl transferase activity



of pol  $\beta$  resides in the 31 kDa carboxyl-terminal polymerase domain. A helix–hairpin–helix structural motif is found in each domain and interacts with the DNA backbone in a non-sequence-dependent manner on opposite sides of gapped DNA. Genomic mutations that alter DNA repair systems are a common feature of cancer cells, and changes in the DNA repair enzyme pol  $\beta$  have been identified in several cancers.<sup>3–5,9,12</sup> A leucine to proline change at residue 22 of pol  $\beta$  was isolated from a gastric carcinoma.<sup>9</sup> The change is situated in the middle of  $\alpha$ -helix A in the amino-terminal LD and forms part of a hydrophobic core. The catastrophic structural effect resulting from the L22P mutation was not totally unexpected. It is well-known that proline residues disfavor interior positions in  $\alpha$ -helices;<sup>40</sup> in the referenced study, the authors were not able to identify any examples of  $\alpha$ -helices containing proline at an interior position. An analogous unfolding effect has been reported to result from the introduction of a T62P substitution in  $\alpha$ -helix A of the model enzyme, staphylococcal nuclease.<sup>20</sup> These profound perturbations highlight the delicate balance that exists between the folded and unfolded states of proteins. The ability of single- or double-stranded DNA to partially rescue the conformation of the unfolded lyase domain was, however, unexpected. Apparently, the binding energy is able to provide some but not all of the energy required to compensate for the destabilizing effect of the mutation. Crystallographic structures of pol  $\beta$ -DNA binary complexes indicate that the short downstream fragment of gapped DNA interacts with residues on  $\alpha$ -helices B–D, but not directly with helix A. An even stronger effect might have been observed if the DNA interacted directly with residues on this helix.

In this series of solution NMR studies, the Met18 methyl resonance was found to provide a particularly useful readout for the structural status of the LD, both in isolation and in the full-length protein. From the perspective of Met18, both pol  $\beta$ (L22P) and the LD(L22P) behave as bistable systems, with folded and unfolded fractions that are dependent on the presence of single- or double-stranded DNA. Additionally, the folded/unfolded ratio can also be influenced by other environmental factors such as TMAO. In both cases, the exchange between the folded and unfolded states is apparently slow on the NMR time scale, consistent with an interconversion rate below  $\sim 10^6$  s<sup>-1</sup>. The NMR data presented here indicate that the conformational rescue by DNA is based more on its effective stabilization of the folded LD, while the effect of the TMAO results more from its destabilization of the unfolded LD, as has been observed for other proteins.<sup>18,19,35</sup> Thus, the DNA complex with LD(L22P) appears to provide a closer approximation of the wild-type structure. The ability of the TMAO to enhance the activity of pol  $\beta$ (L22P) indicates that there is some cooperativity between the effects of the cosolvent and the substrate. A reasonable interpretation of this result is that the TMAO stabilizes a conformational ensemble that more closely approximates that of the wild-type enzyme, providing a more substrate-accommodating binding site than the structure with an unfolded LD.

In contrast with the analysis based on the methionine resonances, a <sup>1</sup>H–<sup>15</sup>N HSQC spectrum of the [U-<sup>15</sup>N]LD-(L22P) indicates that even 3 M TMAO is unable to compensate for the effects of the L22P mutation (Figure S1 of the Supporting Information). The more dynamic structure of the LD(L22P) indicated by the <sup>1</sup>H–<sup>15</sup>N HSQC spectrum is consistent with the broader Met18 methyl resonance of the folded structure observed in the presence of TMAO (Figure

3D). For this system, the observation of two resolved Met18 resonances provides a useful basis for determining the ratio of folded to unfolded states, while the amide HSQC spectrum does not lend itself to such a direct evaluation.

Two models are generally considered for ligand-assisted protein folding: (1) an induced-fit model in which binding of a ligand to a catalytically inactive conformation results in a catalytically active conformation<sup>41</sup> and (2) a conformational selection model in which binding of a ligand to a minor population exhibiting a relatively high ligand affinity shifts the equilibrium to a folded state.<sup>42</sup> The substrate-induced rescue of full-length pol  $\beta$ (L22P) is consistent with the induced-fit model. However, because the ligand-binding competent population is expected to be small and difficult to detect, some degree of conformational selection cannot be fully discounted. More recently, an extension of the conformational selection model that also incorporates an induced-fit component has been proposed.<sup>43</sup> Although for DNA polymerases, induced fit generally has been discussed in terms of substrate specificity (i.e., right and wrong nucleotide selection),<sup>44</sup> binding of a ligand to unfolded or partially unfolded proteins (e.g., intrinsically disordered proteins) alters their conformational distribution, and this type of ligand-induced folding is significant for many cellular interactions. Initial DNA gap binding by pol  $\beta$  is expected to occur through the LD that recognizes the 5'-phosphate in gapped DNA.<sup>38</sup> In the absence of a folded LD, the level of binding of DNA to pol  $\beta$ (L22P) is reduced, thereby reducing the catalytic activities even in the presence of DNA. In addition, nucleotide binding is also affected. Generally, the binary DNA complex exists in an open conformation where the nucleotide binding pocket is exposed. Binding of a nucleotide results in a conformational change (repositioning of the N-subdomain of the polymerase domain) that provides the enzyme the opportunity to probe proper base pair geometry. Normally, the LD forms intimate contacts with the N-subdomain that are necessary for a stable ternary complex. In the absence of a properly folded LD, the catalytic efficiencies for nucleotide insertion and nucleotide binding are strongly compromised (Table 1).

It previously has been suggested that the L22P pol  $\beta$  variant can produce a mutator phenotype,<sup>6</sup> and this could be a direct consequence of the expression of a variant that exhibits low fidelity. It is already known that many of the cancer-associated variants of pol  $\beta$  that produce structural perturbations much less profound than those produced by the L22P mutation can significantly reduce polymerase fidelity. The very low activity of the variant and its limited ability to insert incorrect nucleotides suggest that poor fidelity is not the direct cause of a mutator phenotype in this case, as the fidelity of the variant in the presence of TMAO was similar to that of the wild-type enzyme. Alternatively, a reduced level of DNA repair, expected because of the loss of activity, and/or the possibility that the variant interferes with DNA repair (trans-dominant inhibition), e.g., by forming inactive complexes with XRCC1, may be expected to indirectly increase the level of mutations.

## ■ ASSOCIATED CONTENT

### ● Supporting Information

Effects of 2 and 3 M TMAO on the <sup>1</sup>H–<sup>15</sup>N HSQC spectra of the LD(L22P) (Figure S1). This material is available free of charge via the Internet at <http://pubs.acs.org>.



## AUTHOR INFORMATION

### Corresponding Author

\*Address: 111 TW Alexander Dr., P.O. Box 12233, MD MR-01, Research Triangle Park, NC 27709. E-mail: london@niehs.nih.gov. Phone: (919) 541-4879.

### Funding

This research was supported by the Intramural Research Program of the National Institutes of Health, National Institute of Environmental Health Sciences (NIEHS), under Research Project Z01-ES050147 to R.E.L. and Research Projects Z01-ES050158 and Z01-ES050159 to S.H.W. E.F.D. is supported by the National Institutes of Health, NIEHS, under Delivery Order HHSN273200700046U.

### Notes

The authors declare no competing financial interest.

## ACKNOWLEDGMENTS

We are grateful to Virginia Bass and Cassandra Smith for technical assistance in the preparations of the pol  $\beta$  variants used in these studies.

## ABBREVIATIONS

5'-dRP, 5-deoxyribose phosphate; BER, base excision repair; DTT, dithiothreitol; LD, lyase domain; pol  $\beta$ , DNA polymerase  $\beta$ ; TMAO, trimethylamine N-oxide; XRCC1, X-ray cross complementing group 1 protein.

## REFERENCES

- Hoeijmakers, J. H. J. (2001) Genome maintenance mechanisms for preventing cancer. *Nature* 411, 366–374.
- Hoeijmakers, J. H. J. (2009) Molecular Origins of Cancer DNA Damage, Aging, and Cancer. *N. Engl. J. Med.* 361, 1475–1485.
- Starcevic, D., Dalal, S., and Sweasy, J. B. (2004) Is there a link between DNA polymerase  $\beta$  and cancer? *Cell Cycle* 3, 998–1001.
- Donigan, K. A., Sun, K. W., Nemec, A. A., Murphy, D. L., Cong, X. Y., Northrup, V., Zelterman, D., and Sweasy, J. B. (2012) Human POLB Gene Is Mutated in High Percentage of Colorectal Tumors. *J. Biol. Chem.* 287, 23830–23839.
- Wallace, S. S., Murphy, D. L., and Sweasy, J. B. (2012) Base excision repair and cancer. *Cancer Lett.* 327, 73–89.
- Dalal, S., Chikova, A., Jaeger, J., and Sweasy, J. B. (2008) The Leu22Pro tumor-associated variant of DNA polymerase  $\beta$  is dRP lyase deficient. *Nucleic Acids Res.* 36, 411–422.
- Dalal, S., Hile, S., Eckert, K. A., Sun, K., Starcevic, D., and Sweasy, J. B. (2005) Prostate-cancer-associated 1260M variant of DNA polymerase  $\beta$  is a sequence-specific mutator. *Biochemistry* 44, 15664–15673.
- Dalal, S., Kosa, J. L., and Sweasy, J. B. (2004) The D246V mutant of DNA polymerase  $\beta$  misincorporates nucleotides: Evidence for a role for the flexible loop in DNA positioning within the active site. *J. Biol. Chem.* 279, 577–584.
- Iwanaga, A., Ouchida, M., Miyazaki, K., Hori, K., and Mukai, T. (1999) Functional mutation of DNA polymerase  $\beta$  found in human gastric cancer: Inability of the base excision repair in vitro. *Mutat. Res.* 435, 121–128.
- Lang, T. M., Dalal, S., Chikova, A., DiMaio, D., and Sweasy, J. B. (2007) The E295K DNA polymerase  $\beta$  gastric cancer-associated variant interferes with base excision repair and induces cellular transformation. *Mol. Cell. Biol.* 27, 5587–5596.
- Lang, T. M., Maitra, M., Starcevic, D., Li, S. X., and Sweasy, J. B. (2004) A DNA polymerase  $\beta$  mutant from colon cancer cells induces mutations. *Proc. Natl. Acad. Sci. U.S.A.* 101, 6074–6079.
- An, C. L., Chen, D. S., and Makridakis, N. M. (2011) Systematic Biochemical Analysis of Somatic Missense Mutations in DNA

Polymerase  $\beta$  Found in Prostate Cancer Reveal Alteration of Enzymatic Function. *Hum. Mutat.* 32, 415–423.

(13) Kirby, T. W., DeRose, E. F., Cavanaugh, N. A., Beard, W. A., Shock, D. D., Mueller, G. A., Wilson, S. H., and London, R. E. (2011) Metal-induced DNA translocation leads to DNA polymerase conformational activation. *Nucleic Acids Res.* 40, 2974–2983.

(14) Li, Y. L., Gridley, C. L., Jaeger, J., Sweasy, J. B., and Schlick, T. (2012) Unfavorable Electrostatic and Steric Interactions in DNA Polymerase  $\beta$  E295K Mutant Interfere with the Enzyme's Pathway. *J. Am. Chem. Soc.* 134, 9999–10010.

(15) Taylor, R. M., Wickstead, B., Cronin, S., and Caldecott, K. W. (1998) Role of a BRCT domain in the interaction of DNA ligase III- $\alpha$  with the DNA repair protein XRCC1. *Curr. Biol.* 8, 877–880.

(16) Cuneo, M. J., and London, R. E. (2010) Oxidation state of the XRCC1 N-terminal domain regulates DNA polymerase  $\beta$  binding affinity. *Proc. Natl. Acad. Sci. U.S.A.* 107, 6805–6810.

(17) Wang, L. M., Bhattacharyya, N., Rabi, T., Wang, L., and Banerjee, S. (2007) Mammary carcinogenesis in transgenic mice expressing a dominant-negative mutant of DNA polymerase  $\beta$  in their mammary glands. *Carcinogenesis* 28, 1356–1363.

(18) Wang, A. J., and Bolen, D. W. (1997) A naturally occurring protective system in urea-rich cells: Mechanism of osmolyte protection of proteins against urea denaturation. *Biochemistry* 36, 9101–9108.

(19) Street, T. O., Bolen, D. W., and Rose, G. D. (2006) A molecular mechanism for osmolyte-induced protein stability. *Proc. Natl. Acad. Sci. U.S.A.* 103, 13997–14002.

(20) Baskakov, I., and Bolen, D. W. (1998) Forcing thermodynamically unfolded proteins to fold. *J. Biol. Chem.* 273, 4831–4834.

(21) Bose-Basu, B., DeRose, E. F., Kirby, T. W., Mueller, G. A., Beard, W. A., Wilson, S. H., and London, R. E. (2004) Dynamic characterization of a DNA repair enzyme: NMR studies of [methyl- $^{13}\text{C}$ ]methionine-labeled DNA polymerase  $\beta$ . *Biochemistry* 43, 8911–8922.

(22) John, B. K., Plant, D., and Hurd, R. E. (1993) Improved proton-detected heteronuclear correlation using gradient-enhanced Z And ZZ filters. *J. Magn. Reson.* 101, 113–117.

(23) Delaglio, F., Grzesiek, S., Vuister, G. W., Zhu, G., Pfeifer, J., and Bax, A. (1995) NMRPipe: A multidimensional spectral processing system based on UNIX pipes. *J. Biomol. NMR* 6, 277–293.

(24) Johnson, B. A., and Blevins, R. A. (1994) NMRView: A computer-program for the visualization and analysis of NMR data. *J. Biomol. NMR* 4, 603–614.

(25) Zhu, G., and Bax, A. (1992) Improved linear prediction of damped NMR signals using modified forward backward linear prediction. *J. Magn. Reson.* 100, 202–207.

(26) Yang, D. W., and Kay, L. E. (1999) Improved (HN)-H-1-detected triple resonance TROSY-based experiments. *J. Biomol. NMR* 13, 3–10.

(27) Mueller, G. A., DeRose, E. F., Kirby, T. W., and London, R. E. (2007) NMR assignment of polymerase  $\beta$  labeled with H-2, C-13, and N-15 in complex with substrate DNA. *Biomol. NMR Assignments* 1, 33–35.

(28) Tugarinov, V., and Kay, L. E. (2003) Ile, Leu, and Val methyl assignments of the 723-residue malate synthase G using a new labeling strategy and novel NMR methods. *J. Am. Chem. Soc.* 125, 13868–13878.

(29) Beard, W. A., Shock, D. D., and Wilson, S. H. (2004) Influence of DNA structure on DNA polymerase  $\beta$  active site function: Extension of mutagenic DNA intermediates. *J. Biol. Chem.* 279, 31921–31929.

(30) Wishart, D. S., Bigam, C. G., Holm, A., Hodges, R. S., and Sykes, B. D. (1995) H-1, C-13 and N-15 Random Coil NMR Chemical-Shifts of the Common Amino-Acids. 1. Investigations of Nearest-Neighbor Effects. *J. Biomol. NMR* 5, 67–81.

(31) Bose-Basu, B., DeRose, E. F., Kirby, T. W., Mueller, G. A., Beard, W. A., Wilson, S. H., and London, R. E. (2004) Dynamic characterization of a DNA repair enzyme: NMR studies of [methyl- $^{13}\text{C}$ ]methionine-labeled DNA polymerase  $\beta$ . *Biochemistry* 43, 8911–8922.

- (32) Kirby, T. W., DeRose, E. F., Beard, W. A., Wilson, S. H., and London, R. E. (2005) A thymine isostere in the templating position disrupts assembly of the closed DNA polymerase  $\beta$  ternary complex. *Biochemistry* 44, 15230–15237.
- (33) Prasad, R., Kumar, A., Widen, S. G., Casasfinet, J. R., and Wilson, S. H. (1993) Identification of Residues in the Single-Stranded DNA-Binding Site of the 8-Kda Domain of Rat DNA Polymerase- $\beta$  by UV Cross-Linking. *J. Biol. Chem.* 268, 22746–22755.
- (34) Gao, G. H., DeRose, E. F., Kirby, T. W., and London, R. E. (2006) NMR determination of lysine  $pK_a$  values in the pol  $\lambda$  lyase domain: Mechanistic implications. *Biochemistry* 45, 1785–1794.
- (35) Jaravine, V. A., Rathgeb-Szabo, K., and Alexandrescu, A. T. (2000) Microscopic stability of cold shock protein A examined by NMR native state hydrogen exchange as a function of urea and trimethylamine N-oxide. *Protein Sci.* 9, 290–301.
- (36) Freudenthal, B. D., Beard, W. A., Shock, D. D., and Wilson, S. H. (2013) Observing a DNA Polymerase Choose Right from Wrong. *Cell* 154, 157–168.
- (37) Jaju, M., Beard, W. A., and Wilson, S. H. (1995) Human-Immunodeficiency-Virus Type-1 Reverse-Transcriptase: 3'-Azidodeoxythymidine 5'-Triphosphate Inhibition Indicates 2-Step Binding for Template-Primer. *J. Biol. Chem.* 270, 9740–9747.
- (38) Prasad, R., Beard, W. A., and Wilson, S. H. (1994) Studies of Gapped DNA Substrate-Binding by Mammalian DNA-Polymerase- $\beta$ : Dependence on 5'-Phosphate Group. *J. Biol. Chem.* 269, 18096–18101.
- (39) Beard, W. A., and Wilson, S. H. (2006) Structure and mechanism of DNA polymerase  $\beta$ . *Chem. Rev.* 106, 361–382.
- (40) Chou, P. Y., and Fasman, G. D. (1974) Conformational Parameters for Amino-Acids in Helical,  $\beta$ -Sheet, and Random Coil Regions Calculated from Proteins. *Biochemistry* 13, 211–222.
- (41) Koshland, D. E. (1958) Application of a Theory of Enzyme Specificity to Protein Synthesis. *Proc. Natl. Acad. Sci. U.S.A.* 44, 98–104.
- (42) Tsai, C. J., Kumar, S., Ma, B. Y., and Nussinov, R. (1999) Folding funnels, binding funnels, and protein function. *Protein Sci.* 8, 1181–1190.
- (43) Csermely, P., Palotai, R., and Nussinov, R. (2010) Induced fit, conformational selection and independent dynamic segments: An extended view of binding events. *Trends Biochem. Sci.* 35, 539–546.
- (44) Johnson, K. A. (2008) Role of induced fit in enzyme specificity: A molecular forward/reverse switch. *J. Biol. Chem.* 283, 26297–26301.